Active Low-Pass Filter

Jaeho Cho
ECE444 - Bioinstrumentation and Sensing
The Cooper Union for the Advancement of Science and Art
New York City, NY
jaeho.cho@cooper.edu

***Abstract*—This project explores the design and implementation of a second-order active low-pass filter using the Sallen-Key topology. The filter is designed to have a Butterworth response, which provides a maximally flat frequency response in the passband. The results are compared with theoretical predictions, and the implications of component tolerances and op-amp characteristics on the filter's performance are discussed.**

***Index Terms*—Sallen-Key, Butterworth**

I. Introduction

The Sallen-Key topology is a popular active low-pass filter design that utilizes operational amplifiers (op-amps) to achieve a desired frequency response. The design explored in this project is a second-order low-pass filter with a Butterworth response, which provides a maximally flat frequency response in the passband.

A. Circuit Analysis

a) *Nodal Analysis:* Examining the circuit illustrated in Fig. 1, KCL can be applied at node A to get

$$\frac{V_{\text{in}} - V_A}{R_1} = \frac{V_A - V_B}{R_2} + sC_1(V_A - V_{\text{out}}) \tag{1}$$

and at node B

$$\frac{V_A - V_B}{R_2} = sC_2 V_B \tag{2}$$

which can be solved for V_A:

$$V_A = V_B(1 + sR_2C_2). \tag{3}$$

This allows for the substitution of V_A into equation (1), giving

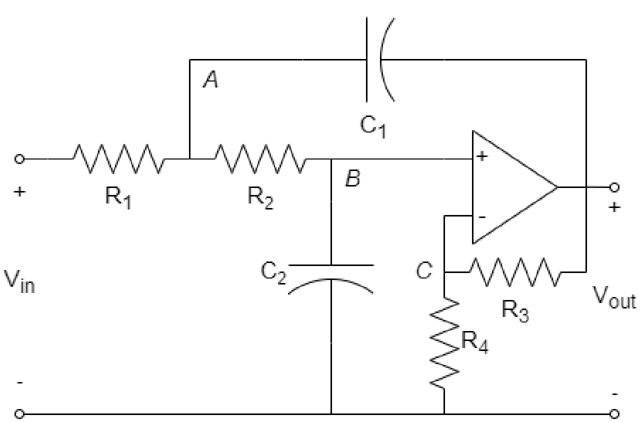

Fig. 1: Sallen-Key topology for the active low-pass filter.

$$\begin{aligned}&\frac{V_{\text{in}} - V_B(1 + sR_2C_2)}{R_1} \\ &= \frac{V_B(1 + sR_2C_2) - V_B}{R_2} + sC_1[V_B(1 + sR_2C_2) - V_{\text{out}}]\end{aligned} \tag{4}$$

The first term in the right side of the equation simplifies to sC_2V_B thus giving

$$\begin{aligned}&\frac{V_{\text{in}} - V_B(1 + sR_2C_2)}{R_1} \\ &= sC_2V_B + sC_1[V_B(1 + sR_2C_2) - V_{\text{out}}]\end{aligned} \tag{5}$$

b) *Op–Amp Feedback and Gain:* A voltage divider (R_3, R_4) connected from the output of the op-amp to the inverting input provides a gain of

$$K = 1 + \frac{R_3}{R_4} \tag{6}$$

where the output voltage is given by

$$V_{\text{out}} = KV_B. \tag{7}$$

Substituting (7) into (5) gives

$$\begin{aligned}&\frac{V_{\text{in}} - V_B(1 + sR_2C_2)}{R_1} \\ &= sC_2V_B + sC_1[V_B(1 + sR_2C_2 - K)].\end{aligned} \tag{8}$$

Equation (8) can finally be rearranged into the transfer function

$$\frac{V_{\text{out}}}{V_{\text{in}}} = \frac{K}{1 + sA + s^2B}. \tag{9}$$

where

$$\begin{aligned}A &= R_2C_2 + R_1C_2 + R_1C_1(1 - K), \\ B &= R_1R_2C_1C_2.\end{aligned} \tag{10}$$

c) *Normalizing to the Standard Second-Order Form:* A standard second–order low–pass filter has the form

$$H(s) = \frac{K\omega_0^2}{s^2 + \frac{\omega_0}{Q}s + \omega_0^2}. \tag{11}$$

Compared with equation (9), the quadratic coefficient from (10) is $B = R_1R_2C_1C_2$. Thus the natural frequency ω_0 must satisfy

$$\omega_0^2 = \frac{1}{B} = \frac{1}{R_1R_2C_1C_2}. \tag{12}$$

It is now convenient to rewrite the denominator of (9) by factoring out B:

$$
\begin{aligned}
&1 + sA + s^2 B \\
&= B\left[s^2 + \frac{A}{B}s + \frac{1}{B}\right] \\
&= B\left[s^2 + \frac{A}{B}s + \omega_0^2\right].
\end{aligned} \tag{13}
$$

Thus, the transfer function becomes

$$
\frac{V_{\text{out}}}{V_{\text{in}}} = \frac{K}{B}\frac{1}{s^2 + \frac{A}{B}s + \omega_0^2}. \tag{14}
$$

Multiplying numerator and denominator by ω_0^2 (noting that $\omega_0^2 B = 1$ by (12)) gives

$$
\frac{V_{\text{out}}}{V_{\text{in}}} = \frac{K\omega_0^2}{s^2 + \frac{A}{B}s + \omega_0^2}. \tag{15}
$$

By comparing with the standard form it is clear that

$$
\frac{\omega_0}{Q} = \frac{A}{B}. \tag{16}
$$

Substitute back A and B:

$$
\frac{\omega_0}{Q} = \frac{R_2C_2 + R_1C_2 + R_1C_1(1-K)}{R_1R_2C_1C_2}. \tag{17}
$$

Since $\omega_0 = 1/\sqrt{R_1R_2C_1C_2}$,

$$
\frac{1}{Q} = \frac{R_2C_2 + R_1C_2 + R_1C_1(1-K)}{R_1R_2C_1C_2}\sqrt{R_1R_2C_1C_2}. \tag{18}
$$

Rearranging gives

$$
\frac{1}{Q} = \sqrt{\frac{R_2C_2}{R_1C_1}} + \sqrt{\frac{R_1C_2}{R_2C_1}} + (1-K)\sqrt{\frac{R_1C_1}{R_2C_2}}. \tag{19}
$$

II. Methodology

A. Design

Given the common constraints of equal-valued capacitors and a gain of 2, the values of the components were chosen to provide a quality factor Q of $1/\sqrt{2}$ for a critically damped response. The cutoff frequency was left as a free parameter to be determined by the component values, which were chosen for simplicity and availability.

Given these goals, equation (19) constrains the values of the resistors

$$
\begin{aligned}
\sqrt{2} &= \sqrt{\frac{R_2}{R_1}} + \sqrt{\frac{R_1}{R_2}} - 1\sqrt{\frac{R_1}{R_2}}, \\
R_2 &= 2R_1.
\end{aligned} \tag{20}
$$

Deciding $R_1 = 10\ \text{k}\Omega$ constrains all the other component values given in Table I.

From the relation given in equation (12), the cutoff frequency is expected to be $1/\left(2\pi\sqrt{R_1R_2C_1C_2}\right) = 112.54$ Hz.

The circuit was built on a breadboard shown

B. Experimental Analysis

The frequency response was measured using a function generator and an oscilloscope. The function generator was set to output a sine wave with a peak-to-peak voltage of 1V, and the frequency was varied from 2 Hz to 10 kHz in qualitatively decided intervals. The output peak-to-peak voltage was measured at each frequency and recorded.

The roll-off rate was determined by plotting Δ Gain $/\Delta$ Frequency and qualitatively estimating the roll-off rate in the stopband.

TABLE I: Theoretical Component Values

Component	Ideal	Measured
R_1	10 kΩ	10.0280 kΩ
R_2	20 kΩ	20.083 kΩ
R_3	24 kΩ	23.949 kΩ
R_4	24 kΩ	23.689 kΩ
C_1	100 nF	98.4265 nF
C_2	100 nF	98.0168 nF

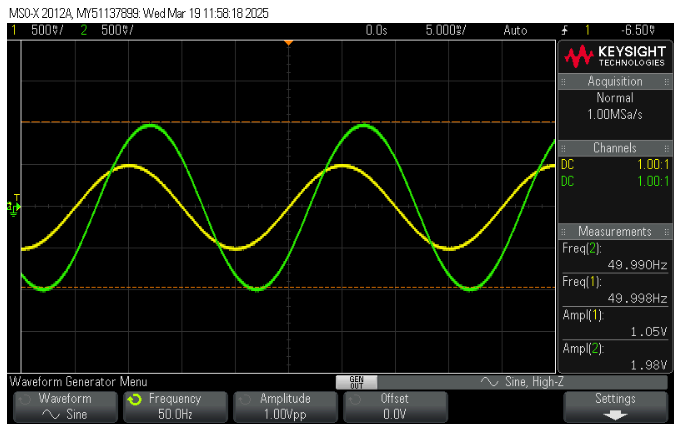

Fig. 2: Oscilloscope Measurement at 50 Hz

III. Results

The power supply was set to 9V, and the circuit pulled a current of 0.02A i.e. power consumption was 0.18W.

The measured frequency response is illustrated alongside the theoretical butterworth frequency response in Fig. 3 and the measured values are given in Table II. The −3 dB point is located at approximately 125 Hz, which is higher than the expected cutoff frequency of 112.54 Hz.

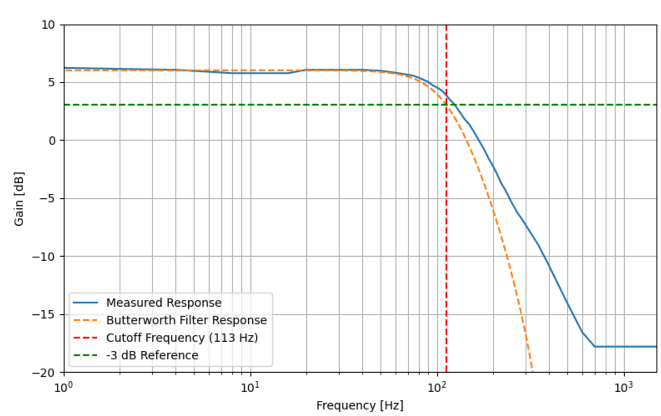

Fig. 3: Measured and Theoretical Frequency Response

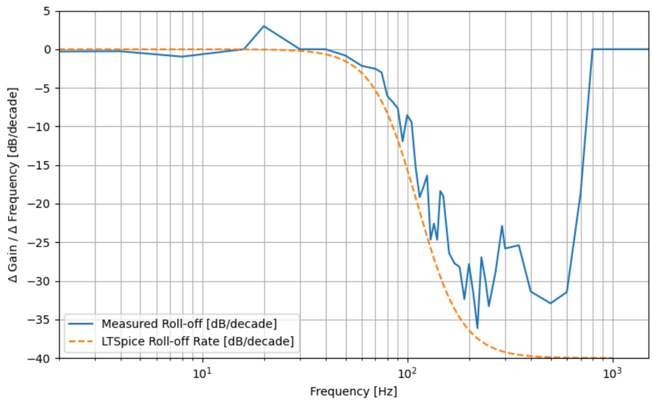

Fig. 4: Measured and Simulated Roll-off Rate

Looking at Fig. 4, the roll-off rate appears to be approximately -30 dB / decade in the stopband, which falls short of the expected behavior of a second-order low-pass filter which should be -40 dB / decade.

IV. Discussion

The cutoff frequency was higher than expected, which can be attributed to the tolerances of the components used, e.g. the capacitors were 98.4265 nF and 98.0168 nF instead of the expected 100 nF which increases the cutoff frequency.

The roll-off rate was also lower than expected, which can be attributed to the fact that the LF411 op-amp [1] used in the circuit is not ideal and has a finite gain-bandwidth product. This means that the gain of the op-amp decreases at higher frequencies, which affects the roll-off rate of the filter. The roll-off rate of the LTSpice simulation is illustrated in Fig. 4 and it can be observed that at the experimental roll-off closely follows the LTSpice simulation up to around 200 Hz where the experimental roll-off rate begins to slow down, which given the finite gain-bandwidth product of the op-amp supports the expectation that the roll-off rate will not be as steep as the ideal -40 dB / decade.

V. Appendix

A. Breadboard

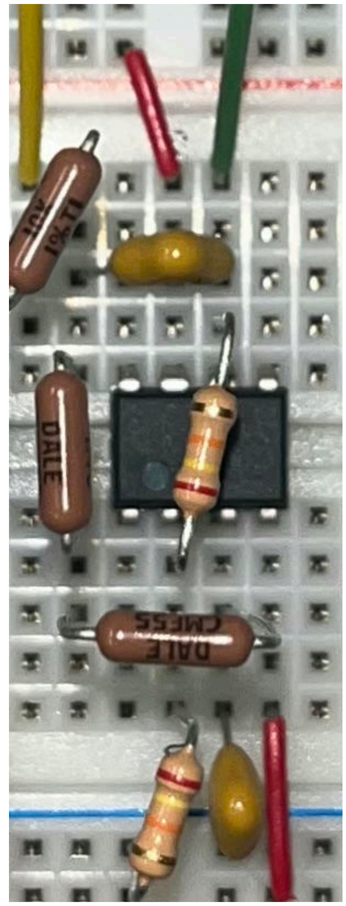

Fig. 5: Breadboard Circuit

B. Simulation

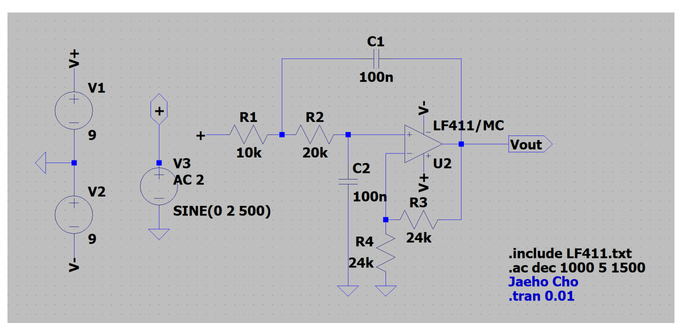

Fig. 6: LTSpice Circuit

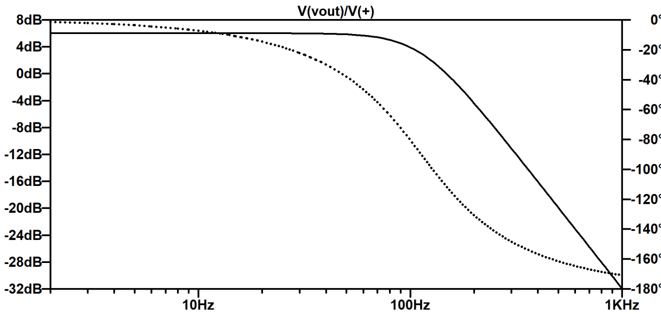

Fig. 7: LTSpice Frequency Response

C. *Raw Data*

TABLE II: Measured Frequency Response Values

Frequency [Hz]	V_in [V]	V_out [V]	Gain	Gain [dB]
2	1.05	2.13	2.03	6.14
4	1.05	2.11	2.01	6.06
8	1.05	2.04	1.94	5.77
16	1.05	2.04	1.94	5.77
20	1.05	2.11	2.01	6.06
30	1.05	2.11	2.01	6.06
40	1.05	2.11	2.01	6.06
50	1.05	2.09	1.99	5.98
60	1.05	2.05	1.95	5.81
70	1.05	2.01	1.91	5.64
75	1.05	1.99	1.9	5.55
80	1.05	1.95	1.86	5.38
85	1.05	1.91	1.82	5.2
90	1.05	1.87	1.78	5.01
95	1.05	1.81	1.72	4.73
100	1.05	1.77	1.69	4.54
105	1.05	1.73	1.65	4.34
110	1.05	1.67	1.59	4.03
115	1.05	1.6	1.52	3.66
120	1.05	1.54	1.47	3.33
125	1.05	1.49	1.42	3.04
130	1.05	1.42	1.35	2.62
135	1.05	1.36	1.3	2.25
140	1.05	1.3	1.24	1.86
145	1.05	1.26	1.2	1.58
150	1.05	1.22	1.16	1.3
160	1.05	1.12	1.07	0.56
170	1.05	1.03	0.98	-0.17
180	1.05	0.95	0.9	-0.87
190	1.05	0.87	0.83	-1.63
200	1.05	0.81	0.77	-2.25
210	1.05	0.75	0.71	-2.92
220	1.05	0.69	0.66	-3.65
230	1.05	0.65	0.62	-4.17
240	1.05	0.61	0.58	-4.72
250	1.05	0.57	0.54	-5.31
270	1.05	0.51	0.49	-6.27
290	1.05	0.47	0.45	-6.98
300	1.05	0.45	0.43	-7.36
350	1.05	0.37	0.35	-9.06
400	1.05	0.3	0.29	-10.88
500	1.01	0.2	0.2	-14.07
600	1.01	0.15	0.15	-16.56
700	1.01	0.13	0.13	-17.81
800	1.01	0.13	0.13	-17.81
900	1.01	0.13	0.13	-17.81
1000	1.01	0.13	0.13	-17.81
1500	1.01	0.13	0.13	-17.81

References

[1] "LF411 JFET-INPUT OPERATIONAL AMPLIFIER," 1997.